JOC The Journal of Organic Chemistry

Article

pubs.acs.org/joc

Cross- versus Homo-Photocyclodimerization of Anthracene and 2-Anthracenecarboxylic Acid Mediated by a Chiral Hydrogen-Bonding Template. Factors Controlling the Cross-/Homo-Selectivity and Enantioselectivity

Yuko Kawanami,[†] Hiroaki Umehara,[†] Jun-ichi Mizoguchi,[§] Masaki Nishijima,[‡] Gaku Fukuhara,[†] Cheng Yang,[∥] Tadashi Mori,[†] and Yoshihisa Inoue*[,†]

[†]Department of Applied Chemistry and [‡]Office for University-Industry Collaboration, Osaka University, 2-1 Yamadaoka, Suita 565-0871, Japan

[§]Bio/Fine Chemicals Department, Nagase ChemteX, 2-2-3 Murotani, Nishi-ku, Kobe 651-2241, Japan

[∥]College of Chemistry, Sichuan University, Wangjiang Road, Chengdu 610064, People's Republic of China

Supporting Information

ABSTRACT: Competitive cross-/homo-photocyclodimerization of anthracene (AN) and 2-anthracenecarboxylic acid (AC) mediated by a chiral hydrogen-bonding template (TKS) was investigated under various conditions. The cross-photocyclodimerization was favored by a factor of 4−5 at all temperatures and wavelengths examined to afford the AC-AN cross-dimer in 80−84% yield even at AN/AC = 1 and in 98% yield at AN/AC = 10. The enantiomeric excesses (ee's) obtained were 27−47% for the homo-dimers and 21−24% for the cross-dimer. The absolute configuration of the cross-dimer was determined by comparing the experimental and theoretical circular dichroism spectra and further correlated with the *re/si* enantiotopic-face selectivity upon AC-TKS complexation in the ground state. Detailed analyses of the complexation behavior and the fluorescence lifetime and cyclodimerization rate of excited *re/si* complexes revealed that the product's ee is critically controlled not only by the relative abundance of the *re/si* complexes in the ground and excited states but also by their relative photocyclodimerization rate. Crucially, the ground-state thermodynamics and the excited-state kinetics are not synergistic but offsetting in enantiotopic-face selectivity, and the latter overwhelms the former to give the homo- and cross-dimers in modest ee's. Finally, some practical strategies for enhancing the enantioselectivity in chiral template-mediated photochirogenesis have been proposed.

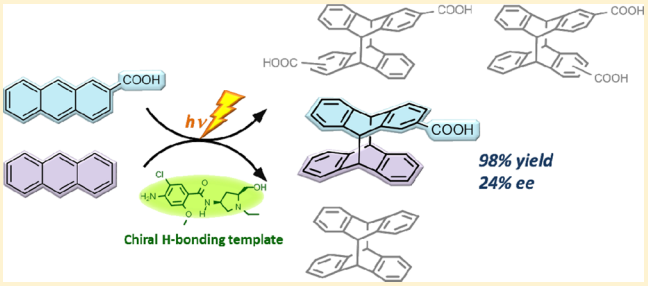

INTRODUCTION

Achieving precise control of a chirogenic process in a short-lived, weakly interacting excited state is an intriguing but challenging task.[1] Recent studies on photochrogenesis have however shown that chiral supramolecular hosts can be used as a convenient yet reliable tool for facilitating excited-state chirality transfer through long-lived closer contacts of prochiral guest substrate(s) with chiral host in both ground and excited states.[2] Thus, a wide variety of chiral supramolecular hosts, such as chirally modified zeolites,[3] hydrogen-bonding templates,[4−6] native and modified cyclodextrins,[7] and proteins,[8] have hitherto been employed for mediating chiral photoreactions to afford satisfactory results in many cases. Despite the apparent success of the supramolecular approach, the chiral recognition/transfer processes in the ground and excited states have rarely been elucidated or discussed in detail at the molecular level, partially due to the more or less sophisticated host structures and the lack of an appropriate set of methodologies for independently evaluating the chiral host−guest interactions and their stereochemical consequences in both states.

Supramolecular photochirogenesis mediated by a hydrogen-bonding template is one of the most suitable systems for closely examining the factors and mechanisms that control the chiral recognition thermodynamics and kinetics in ground and/or excited states. Indeed, we have established a protocol for elucidating the photochirogenesis mechanism by investigating the ground- and excited-state behaviors of the relevant species involved in the enantiodifferentiating [4 + 4] photocyclodimerization of 2-anthracenecarboxylic acid (AC) mediated by a chiral hydrogen-bonding template, 4-amino-5-chloro-2-methoxy-*N*-((2*S*,4*S*)-(1-ethyl-2-hydroxymethyl-4-pyrrolidinyl))-benzamide, or TKS159 (TKS), leading to the formation of four stereoisomeric cyclodimers **1**−**4** via a diastereomeric pair of the 1:1 complex of AC with enantiomeric TKS (Scheme 1).[6b]

Received: January 11, 2013
Published: March 5, 2013

Scheme 1. Complexation of 2-Anthracenecarboxylic Acid (AC) with Chiral Hydrogen-Bonding Template TKS159 To Form a 1:1 AC-TKS Complex with an Open *re* or *si* Face, Followed by Enantiodifferentiating Photocyclodimerization to Stereoisomeric 1−4[a]

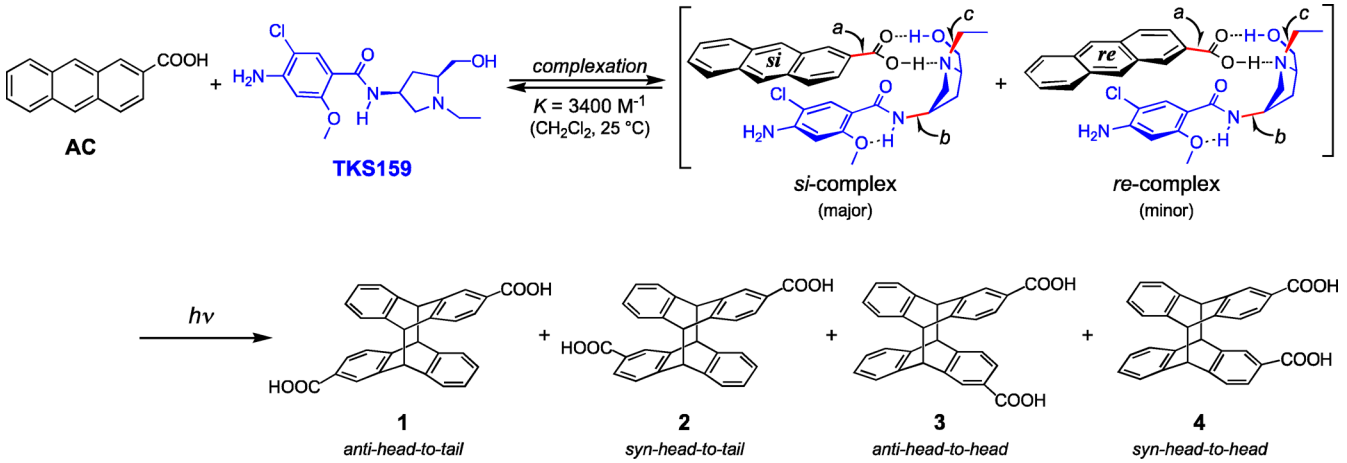

[a]The absolute configurations of chiral **2** and **3** shown above are for the experimentally dominant *P* enantiomers, which are however derived from the less stable (minor) AC-TKS complex with open *re* enantiotopic face (top right); see the text for details.[6b,9] Bonds *a*−*c* shown in red in the complex structures were rotated to create the initial structures in the full conformation search detailed in Results and Discussion.

Scheme 2. Competitive Cross- versus Homo-Photocyclodimerization of 2-Anthracenecarboxlic Acid (AC) and Anthracene (AN) Producing Stereoisomeric AC-AC Homo-Dimers 1−4, the AC-AN Cross-Dimer 5, and the AN-AN Homo-Dimer 6[a]

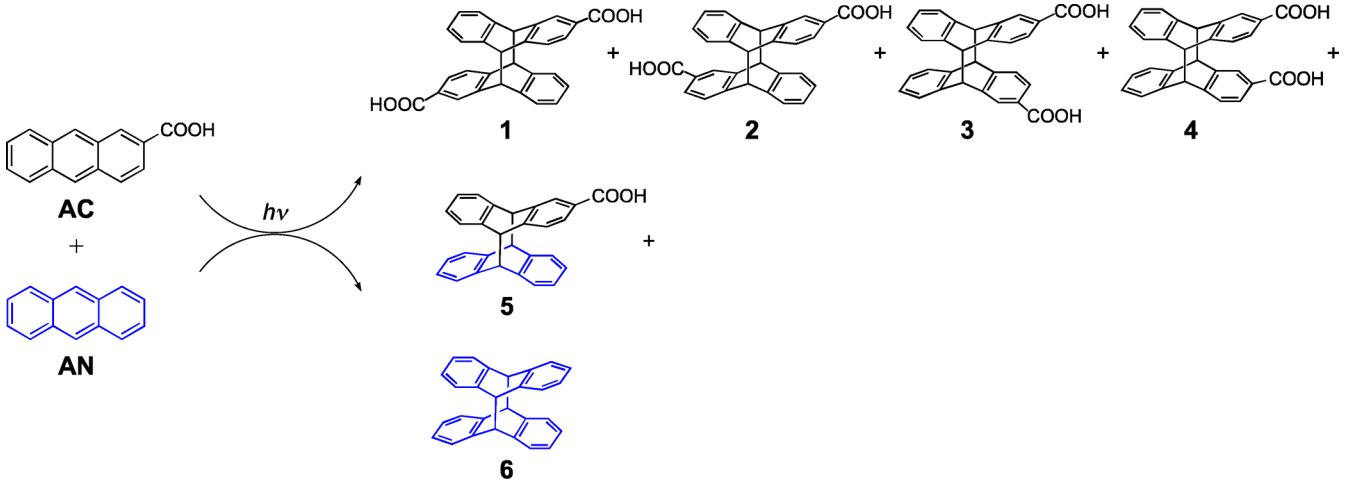

[a]The absolute configurations of **2**, **3**, and **5** shown above are for the experimentally dominant *P* enantiomers.

Nevertheless, it was not feasible at that time to correlate the product's absolute configuration with the enantiotopic-face selectivity upon complexation or subsequent photocyclodimerization, as the absolute configurations of chiral cyclodimers **2** and **3** were determined only recently by comparing the experimental and theoretical circular dichroism (CD) spectra.[9] Also, the diastereomeric pair of the AC-TKS complex was tentatively assumed to have the same photoreactivity, due to our lack of knowledge about their relative fluorescence efficiencies, which however turned out to have led us to an erroneous conclusion on the relative abundance of diastereomeric AC-TKS complexes in the previous study.[6b]

In the present study, we primarily aimed to obtain a single chiral product in the TKS-mediated photocyclodimerization of AC, for which we chose unsubstituted anthracene (AN) as a reaction partner, because (1) AN has no enantiotopic face and hence gives only one chiral cross-dimer **5** upon photocyclodimerization with prochiral AC, (2) AN absorbs at appreciably shorter wavelengths than AC,[10] enabling us to selectively excite AC, and (3) the excited singlet of AN is short-lived compared to that of AC,[10] discouraging its homo- and cross-photocyclodimerization.

In principle, simultaneous photoexcitation of AC and AN affords a mixture of AC-AC homo-dimers **1**−**4**, AC-AN cross-dimer **5**, and AN-AN homo-dimer **6**, as illustrated in Scheme 2. From a mechanistic point of view, the use of a mixed AC-AN system would appear to merely cause more complication, but it is highly advantageous in reality if the AN-AN homophotocyclodimerization is completely suppressed by carefully choosing the irradiation wavelength so as not to excite AN. This is because (1) the enantiomer ratio (er) is not a simple function of the *re*/*si* complex ratio upon AC-AC homophotocyclodimerization, inherently accompanying the "escape" route to achiral **1** and **4** (vide supra), but becomes more straightforward upon AC-AN cross-photocyclodimerization, (2) the reliable analyses of the lifetime and photoreactivity of intervening diastereomeric

dx.doi.org/10.1021/jo302818w | J. Org. Chem. 2013, 78, 3073−3085

excited AC-TKS complexes are feasible by cross-checking the results derived from the homo- and cross-photocyclodimerizations of AC-TKS with AC and AN, and (3) the effect of the steric bulk of AC versus AN upon photocyclodimerization rate is evaluated by comparing the enantiomeric excesses (ee's) of homo- and cross-dimers. Furthermore, by combining the theoretical geometry optimization and energy calculation for each ground-state conformer of diastereomeric AC-TKS complexes with the experimental photophysical and photochemical results obtained, we can elucidate the factors and mechanisms operative in this competitive AC/AN photocyclodimerization system, including the ground-state abundance, excited-state lifetime, and photoreactivity of intervening *re* and *si* AC−TKS complexes.

RESULTS AND DISCUSSION

Preferential Excitation. Since the preferential excitation of one of the two substrates (AC and AN) in the system is advantageous for the mechanism elucidation by reducing the number of excited species involved, we first examined the UV/vis spectra of AC and AN. As shown in Figure 1, both the ^1B_b and $^1L_a/^1L_b$ transitions of AC were significantly red-shifted (and broadened) in comparison to the relevant transitions of parent AN. Thus, the 0−0 band of the ^1L_b transition appears at 400 nm for AC but at 378 nm for AN, permitting selective excitation of AC at 390−420 nm. Although the photoirradiation at 310−370 nm leads to the simultaneous excitation of AC and AN, the preferential excitation of AC seems feasible also at the window of AN absorption, i.e. 270−290 nm, which is however difficult to exploit in practice, as the cyclodimers absorb in the same region.

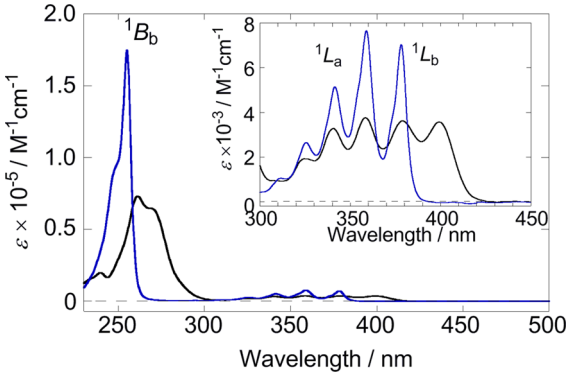

Figure 1. UV/vis spectra of 2-anthracenecarboxylic acid (black) and anthracene (blue) in dichloromethane at 25 °C.

AC-AN Cross-Dimer 5. Since the cross-dimer of AC with AN was not known, we first examined the feasibility of AC-AN cross-photocyclodimerization and then characterized the cross-dimer obtained therefrom. For preparing the cross-dimer, a mixture of AC (1.1 mM) and AN (2.2 mM) was irradiated at >320 nm in methanol at 25 °C. Occasional monitoring of the irradiated solution by UV/vis spectroscopy showed a smooth decrease of the absorbance at longer wavelengths, in particular at >390 nm (Figure S1 in the Supporting Information), indicating that the consumption of AC was faster than that of AN and presumably that preferential cross-cyclodimerization of AC and AN occurred, as supported by the product distribution determined by HPLC analysis.

The irradiated sample was subjected to chiral HPLC analysis on the same tandem (ODS + OJ-RH) column that was used for the analysis of AC cyclodimers **1**−**4** but eluted with acetonitrile/water mixtures of varying compositions from 30/70 to 80/20 (CH_3CN/H_2O) at a gradient of 10% h^{-1}. As shown in the chiral HPLC trances monitored by fluorescence (Figure 2a) and circular dichroism detectors (Figure 2b), the photoreaction was clean (nearly quantitative) and all of the cyclodimers, i.e. AC homo-dimers **1**−**4**, AC-AN cross-dimer **5**, and AN homo-dimer **6**, as well as the enantiomers of chiral dimers **2**, **3**, and **5**, were satisfactorily separated under the conditions employed. Cross-dimer **5** was obtained as the major photoproduct, along with smaller amounts of AC homo-dimers **1**-**4** and a much smaller amount of AN homo-dimer **6**.

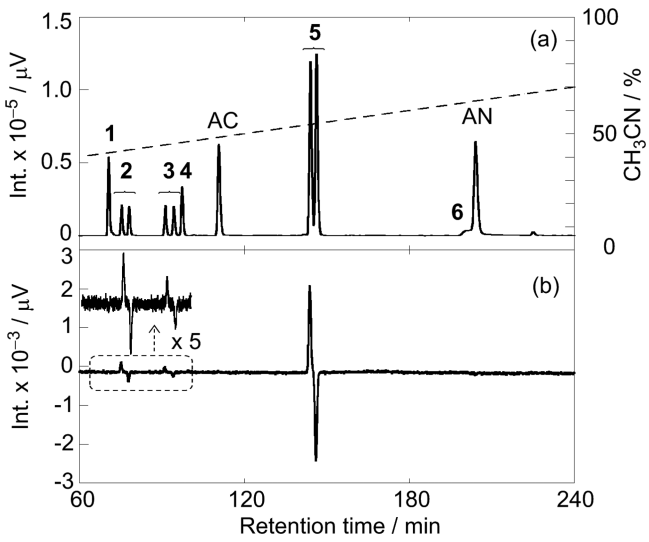

Figure 2. Chiral HPLC traces of the preparative-scale irradiation sample, monitored by (a) fluorescence (λ_{ex} 254 nm, λ_{em} 420 nm)[13] and (b) circular dichroism detection (λ 254 nm): column, Cosmosil 5C$_{18}$-AR-II (Nacalai) + Chiralcel OJ-RH (Daicel) at 35 °C; eluent, a mixture of CH_3CN and H_2O containing 0.1% trifluoroacetic acid (TFA); CH_3CN content varied from 30% to 80% at 10% h^{-1} gradient (dashed line in Figure 2a); flow rate, 0.5 mL min^{-1}.

The racemic cross-dimer **5** thus obtained was isolated from the reaction mixture by preparative HPLC and was subjected to HR-MS and 1D- and 2D-NMR spectral analyses (Figures S2−S8 in the Supporting Information). The structure of **5** rests on the characterization using 2D-NMR techniques, including COSY, NOESY, HSQC, and HMBC, as well as a comparison with the AC homo-dimers[11] and AN homo-dimer.[12]

By using the chemically pure samples of **5** thus isolated and **1** prepared separately,[7,8,6b] the response of the fluorescence detector (λ_{ex} 254 nm, λ_{em} 420 nm)[13] was calibrated for **1** (as a representative of AC homo-dimers **1**−**4**) and AC-AN cross-dimer **5**. This was necessary because the homo- and cross-dimers should respond differently upon fluorescence detection that involves a series of photophysical and photochemical events in the cuvet of a HPLC fluorescence detector: i.e., the initial photoexcitation at 254 nm, the subsequent dissociation regenerating AC and/or AN, the photoexcitation of the AC and/or AN produced, and finally the fluorescence emission therefrom. The calibration experiments performed under conditions comparable to those for the practical HPLC analysis (Figure S9 in the Supporting Information) revealed that the fluorescence detector response for AC-AN dimer **5** is smaller

dx.doi.org/10.1021/jo302818w | J. Org. Chem. 2013, 78, 3073−3085

Table 1. Homo- and Cross-Photocyclodimerization of a 1:1 Mixture of AC and AN upon Excitation at Different Wavelengths[a]

			product distribution/%[d]					
λ_{ex}/nm	AN/AC excitation ratio[b]	AC conversion/%[c]	**1**	**2**	**3**	**4**	**5**	**5**/(**1** + **2** + **3** + **4**)
>320[e,f]	~1	92	5.0	3.7	4.0	3.3	84.0	5.3
360[g]	2	60	6.3	4.2	4.2	3.3	82.0	4.6
390[g]	<0.03	46	5.9	4.1	4.4	3.3	82.3	4.6

[a]Conditions: [AC] = [AN] = 0.1 mM in CH_2Cl_2; irradiated under N_2 for 2 h at 25 °C in a 1 cm cell. [b]Relative efficiency of excitation of AN over AC, evaluated from the (integrated) absorbance at each wavelength (Figure 1). [c]Determined by monitoring the UV/vis spectral change at 400 nm. [d]Determined by chiral HPLC fitted with a fluorescence detector (λ_{ex} 254 nm, λ_{em} 420 nm),[13] the response of which was calibrated by using authentic samples of **1** and **5** isolated from the preparative-scale irradiation samples; for details, see Figure S9 in the Supporting Information. [e]Upon excitation at >320 and 360 nm, a small amount of **6** was formed in <3% and <1% yields, respectively (calculated by using the same calibration factor for **5**) along with **1**−**4**, but no **6** was formed upon excitation at 390 nm. [f]Light source: 500 W ultrahigh pressure Hg lamp fitted with a UV-35 filter. [g]Light source: 300 W Xe lamp fitted with an appropriate interference filter (±10 nm).

by a factor of 2.88 than that for AC homo-dimer **1** (and **2**−**4**); the yield of **5** was corrected for this difference in detector response throughout the work.

Wavelength Effects on Photocyclodimerization of AC and AN. In the present system employing AC and AN as competing substrates, the selective excitation of AC is readily achieved by choosing the irradiation wavelength. Nevertheless, we first examined the effects of excitation wavelength on the product distribution without using the chiral template. Thus, an equimolar mixture of AC and AN (0.1 mM each) was irradiated in dichloromethane under three different wavelength conditions for tuning the relative excitation efficiency of AN over AC: (a) at λ >320 nm for comparable excitation of AC and AN, (b) at 360 nm for 2-fold preferential excitation of AN over AC, and (c) at 390 nm for almost exclusive excitation of AC (Figure 1). The product distributions of **1**−**5** obtained upon excitation at different wavelengths are given in Table 1; the yield of **6** was low (estimated as <3% of total cyclodimers) even upon excitation at >320 nm and at 360 nm, and no **6** was formed upon excitation at 390 nm.

Intriguingly, the AC-AN cross-photocyclodimerization is much more favored than the AC-AC and AN-AN homo-photocyclodimerization, and the excitation wavelength does not appear to affect the cross-/homo-dimer ratio, as can be seen from the practically constant **5**/(**1** + **2** + **3** + **4**) ratios as high as 4.6−5.3 (Table 1). In particular, these results seem unusual considering the twice preferential excitation of AN at 360 nm. The observed product distributions of AC-AC, AC-AN, and AN-AN dimers, i.e. 17/83/~3, deviate far from the statistical 1/2/1 ratio to be realized upon equal excitation and photocyclodimerization of AC and AN, for which the much shorter lifetime of AN (2 ns), relative to AC (15 ns), and the efficient energy transfer from AN to AC are thought to be jointly responsible; more detailed analyses will be given in a later section.

Optical Resolution of 5. Chemically pure *rac*-**5** obtained above was optically resolved by chiral HPLC on a Chiralcel OJ-RH (Daicel) column eluted by a acetonitrile/water/TFA mixture (50/50/0.1) (Figure S10 in the Supporting Information) to give a pair of enantiomers, tentatively assigned as $\mathbf{5}_+$ and $\mathbf{5}_-$ for the first and second fractions, respectively. The optical purities of the resolved samples were determined as >96% ee by using analytical chiral HPLC (Figure S11 in the Supporting Information). The first and second fractions, containing $\mathbf{5}_+$ and $\mathbf{5}_-$, were directly subjected to chiroptical examinations to give the UV/vis and CD spectra and the *g* factor profiles (which are intrinsically corrected for the difference in concentration, as $g = \Delta\varepsilon/\varepsilon$) shown in Figure 3.

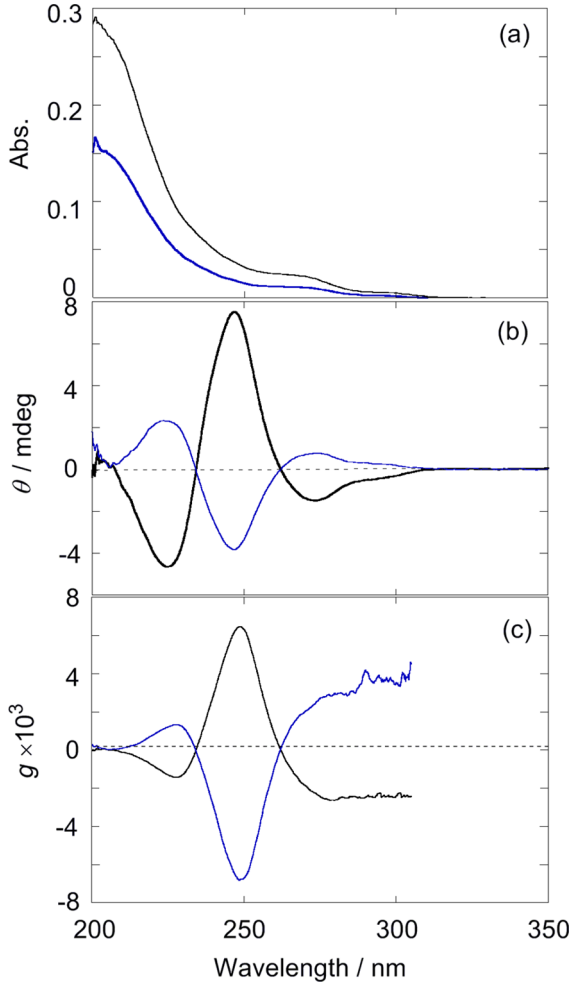

Figure 3. (a) UV/vis spectra, (b) CD spectra, and (c) anisotropy (*g*) factor profiles of $\mathbf{5}_+$ (black) and $\mathbf{5}_-$ (blue) in the HPLC eluent ($CH_3CN/H_2O/CF_3CO_2H$ 50/50/0.1). The concentrations of $\mathbf{5}_+$ and $\mathbf{5}_-$ were estimated as ca. 4.5 and 2.4 μM, respectively, by using the molar extinction coefficient of **5** in a 1/1 mixture of acetonitrile and aqueous 10 mM NaOH solution. Note that the two solutions gave nicely mirror-imaged *g* factor profiles and essentially the same absolute anisotropy factors at the extrema, $g = 6.5 \times 10^{-3}$ for $\mathbf{5}_+$ and -6.7×10^{-3} for $\mathbf{5}_-$ at 249 nm, indicating equally high optical purities.

Theoretical Calculations of the CD Spectra of Enantiomeric Cross-Dimer 5. In the TKS-mediated photocyclodimerization of AC, not only the enantiotopic *re*/*si* face selectivity upon complexation of AC with TKS and but also the relative lifetime and cyclodimerization rate of the diastereo-

dx.doi.org/10.1021/jo302818w | J. Org. Chem. 2013, 78, 3073−3085

meric pair of excited AC-TKS complexes (*re** and *si**) are known to play crucial roles in determining the absolute configurations of enantiomeric **2** and **3** produced.[6b] This means that the ee values of **2** and **3** do not immediately reflect the *re/si* face selectivity upon AC-TKS complexation in the ground state but are critically affected by the excited-state dynamics. In the present cross-photocyclodimerization case, the situation is basically the same for the AC-TKS complexation but the diastereodifferentiating photocyclodimerization mechanism becomes more straightforward, since no "escape" route to achiral cyclodimers (i.e., **1** and **4** in the case of AC-AC photocyclodimerization) exists in the cross-photocyclodimerization of *re/si* AC-TKS complexes with AN. Hence, we are in a better position to elucidate the mechanisms and factors that control the enantiodifferentiating complexation of AC with TKS as well as the diastereodifferentiating photocyclodimerization of AC-TKS complex with AN.

Elucidating the absolute configuration of the major enantiomer of cross-dimer **5** was expected to greatly facilitate the in-depth discussion about the complexation and photocyclodimerization mechanisms from a stereochemical point of view. Since the enantiomer pair of **5** was successfully resolved by chiral HPLC to give the mirror-image CD spectra, we decided to assign the absolute configurations of first-eluted $\mathbf{5}_+$ and second-eluted $\mathbf{5}_-$ by simulating the experimental CD spectra by the approximate coupled cluster calculations at the RI-CC2/TZVPP//DFT-D2-B97-D/TZVP level, which was employed in the theoretical CD calculations of **2** and **3** as well as the chiral cyclodimer of 2,6-anthracenedicarboxylic acid to afford good agreement with the experimental CD spectra.[9] As shown in Figure 4, the theoretical CD spectrum calculated for (1*R*,2*R*,5*S*,6*S*)-**5** at the RI-CC2/TZVPP//DFT-D2-B97-D/TZVP level nicely agreed in shape and relative intensity with the experimental CD spectrum of first-eluted $\mathbf{5}_+$, unequivocally assigning the absolute configuration of AC-AN dimer **5**.

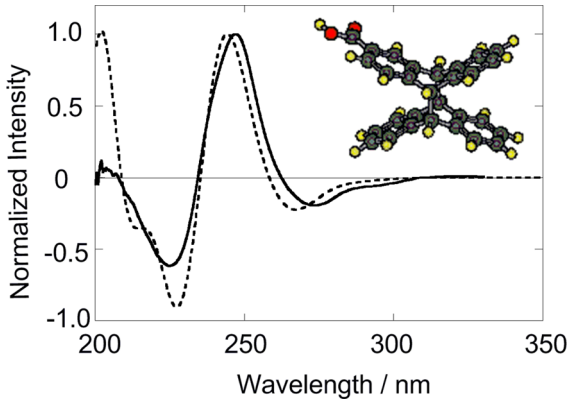

Figure 4. Comparison of normalized experimental (solid line) and theoretical (dotted line) CD spectra of first-eluted AC-AN dimer $\mathbf{5}_+$. The theoretical CD spectrum was red-shifted by 0.2 eV. The theoretical spectrum was calculated for (1*R*,2*R*,5*S*,6*S*)-**5** at the RI-CC2/TZVPP//DFT-D2-B97-D/TZVP level; for the atomic coordinates of dimer $\mathbf{5}_+$, see Table S1 in the Supporting Information.

Geometry Optimization and CD Spectrum Simulation for AC-TKS Complexes. In the present study, we performed a full conformation search for the diastereomeric AC-TKS complexes to evaluate the relative stability of all possible conformational isomers, which allowed us to evaluate the conformer structure and energy. The relevant structures considered by theory were further verified by comparing the solution CD/UV−vis spectra with the theoretical spectra, which were obtained by weighted averaging of all the possible conformers populated at room temperature. The geometries were considered by using the dispersion-corrected DFT method at the DFT-D3-B-LYP/def2-TZVP level. The empirical dispersion correction has been employed as a cost-efficient yet accurate practical tool for calculating medium to large supramolecular systems,[14] and this treatment was mandatory indeed for the current system. The solvent effect was also considered by the conductor-like screening model (COSMO) approach.[15]

We constructed 12 initial structures for the AC-TKS complex by rotating the anthracene ring about the AC's C2−C(═O) bond *a*, the TKS's benzamide moiety about the N(amide)−C4(prolinol) bond *b*, and the prolinol's *N*-ethyl group about the N−C(ethyl) bond *c*, maintaining the hydrogen bond of the amide proton to the methoxy oxygen in TKS and the nine-membered hydrogen-bonding network that dually connects AC with TKS by threading the carboxylic OH to the pyrrolidine N and the prolinol OH to the AC's carbonyl oxygen (Scheme 1).[6a,b]

The geometry optimization was performed for all of these initial structures by using the DFT-D3 method at the B-LYP/def2-TZVP level to afford four conformers, i.e. *si*, *re*, *re′* and *si′*, in the order of increasing energy, each of which had three local minima associated with the *anti*, *gauche*+ (*g*+), and *gauche*− (*g*−) conformations of the *N*-ethyl group; for the DFT-D3-optimized structures of all possible conformers, see Figure S12 in the Supporting Information. As readily recognized from Table 2, the *re′* and *si′* conformers were much higher in energy than *si* and *re*, and the *g*+ conformations of *si* and *re* conformers were substantially less stable than the corresponding *anti* and *g*−. Hence, the four most stable conformers, i.e. *si*(*anti*/*g*−) and *re*(*anti*/*g*−), were subjected to more accurate SCS-MP2 single-point energy calculations[16] using the COSMO solvation model with a dielectric constant set to 8.93 for dichloromethane to afford the relative energies and population shown in Table 2 and the optimized structures in Figure 5.

In the previous paper,[6b] we proposed the *re′* and *si′* conformers as the most plausible structures for the diastereomeric *re* and *si* AC-TKS complexes, respectively. However, the present full conformer search, followed by a geometry optimization, revealed that the *si* and *re* conformers are significantly more stable than the *re′* and *si′* conformers, as shown in Table 2 (and Tables S2 and S3 in the Supporting Information). This is a consequence of the additional hydrogen-bonding interaction of the amide proton with the alcoholic oxygen achieved only in the *si* and *re* conformers, as illustrated in Figure 5 (bold dashed line). Of these two conformers, the *si*(*anti*/*g*−) conformers with an exposed *si* face (*si* complex) are appreciably more stable than the *re*(*anti*/*g*−) conformers with an open *re* face (*re* complex), while the *anti* conformer is consistently more stable than the corresponding *g*− conformer (Table 2). Although the aromatic planes of AC and TKS are apparently less overlapped in the *si*(*anti*/*g*−) conformer than in the *re*(*anti*/*g*−) conformer (Figure 5), the interplane distance is slightly shorter for the former (3.3 Å) than the latter (3.4 Å) (Table S3 in the Supporting Information). Similarly, the interplane distance was shorter for the *re′* (3.5 Å) than for the *si′* conformer (3.6 Å). These results imply that the π stacking may play some role in stabilizing the AC-TKS complex but the apparent π overlap is

dx.doi.org/10.1021/jo302818w | J. Org. Chem. 2013, 78, 3073−3085

Table 2. Relative Energies (ΔE) and Populations (pop) of All Possible Conformers of Stacked AC-TKS Complexes Calculated by the DFT-D3 Method and of Major (Most Stable) Conformers Calculated by the SCS-MP2 and SCS-MP2/COSMO Methods

		DFT-D3/gas phase[a]		SCS-MP2/gas phase[b]		SCS-MP2/COSMO[c]	
conformer	*N*-ethyl	ΔE[d]	pop[e]/%	ΔE[d]	pop[e]/%	ΔE[d]	pop[e]/%
si	*anti*	≡0	44.7	≡0	48.0	≡0	36.2
	g−	0.39	23.0	0.27	30.2	0.10	30.7
	g+	6.0	<0.1	*f*		*f*	
re	*anti*	0.40	22.8	0.72	14.3	0.36	19.8
	g−	0.91	9.5	1.11	7.4	0.59	13.3
	g+	8.1	<0.1	*f*		*f*	
re′	*anti*	6.0	<0.1	*f*		*f*	
	g−	8.0	<0.1	*f*		*f*	
	g+	7.5	<0.1	*f*		*f*	
si′	*anti*	8.1	<0.1	*f*		*f*	
	g−	10.6	<0.1	*f*		*f*	
	g+	9.6	<0.1	*f*		*f*	

[a]Calculated by the DFT-D3 method at the DFT-D3-B-LYP/def2-TZVP level. [b]Calculated at the SCS-MP2/def2-TZVPP//DFT-D3-B-LYP/def2-TZVP level. [c]Calculated at the SCS-MP2/def2-TZVPP//DFT-D3-B-LYP/def2-TZVP level with COSMO solvation model (ε 8.93). [d]In kcal mol^{-1}. [e]Boltzmann distribution at 25 °C. [f]No further calculation was done, as the relative energy calculated by the DFT-D3 method was too high to be populated at ambient temperatures.

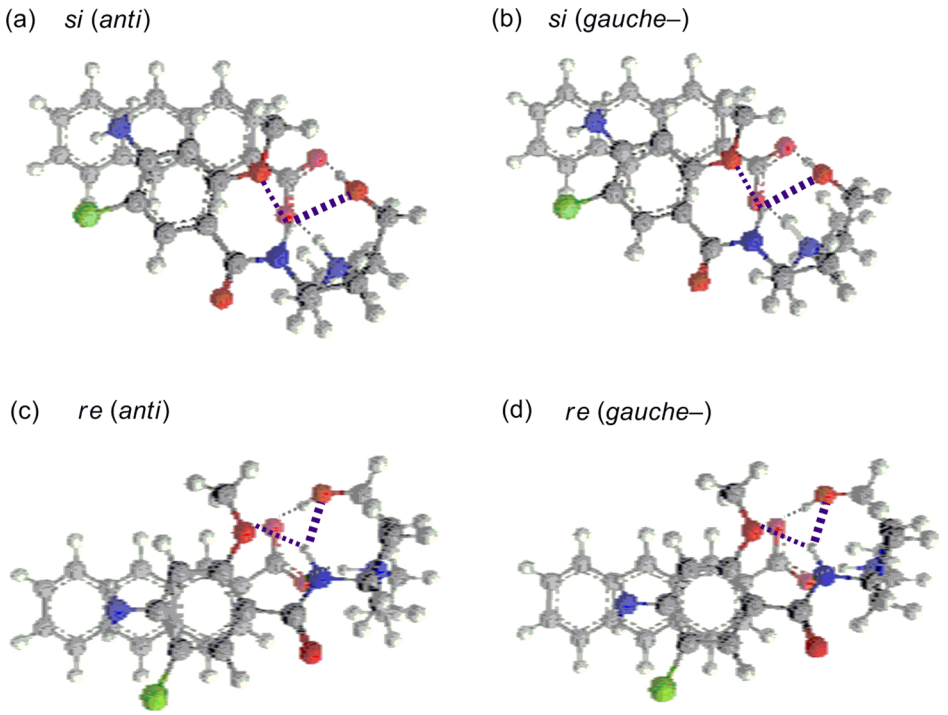

Figure 5. DFT-D3-optimized structures of the four major conformers of the stacked AC-TKS complex, (a) *si*(*anti*), (b) *si*(*g*−), (c) *re*(*anti*), and (d) *re*(*g*−), the first two of which expose the AC *si* face (*si* complex), while the last two expose the *re* face (*re* complex);. For the corresponding front and bottom views, see Figure S13 in the Supporting Information. Note that an additional hydrogen bond (shown as a bold dashed line) connecting the TKS's amide proton and alcohol oxygen is formed in both *si* and *re* conformers to stabilize these significantly more than the *re*′ and *si*′ conformers (shown in Figure S12 in the Supporting Information).

not suitable, or even misleading, as a measure for judging the complex stability. In contrast, all of the hydrogen-bond distances are appreciably shorter for *re*(*anti*) and *si*(*anti*) than for *si*′(*anti*) and *re*′(*anti*) by 0.05−0.18 Å on average (Table S3 in the Supporting Information), which may rationalize the energy differences of 6−8 kcal mol^{-1} between *re*/*si*(*anti*) and *si*′/*re*′(*anti*). Incorporating the solvent effect in energy calculations led to smaller differences in relative energy to appreciably reduce the *si*/*re* ratio from 3.6 under vacuum (SCS-MP2) to 2.0 in dichloromethane (SCS-MP2 with COSMO). The significant instability of all the *g*+ conformers is attributable to the steric hindrance with the pyrrolidine ring and/or the adjacent hydroxymethyl substituent, as the hydrogen-bond length and angle are not very different from those of the *anti* and *g*− conformers (Table S3 in the Supporting Information).

Theoretical CD spectra were calculated for these four stable conformers, i.e. *si*(*anti*/*g*−) and *re*(*anti*/*g*−), at the RI-CC2/def2-TZVPP level to give the results shown in Figure 6a; all the spectra are shown as obtained by calculations (not shifted or scaled). The *si*(*anti*) and *si*(*g*−) conformers afforded very similar CD spectra, exhibiting intense negative Cotton effects at the ^1B_b band and much smaller positive and negative peaks at

dx.doi.org/10.1021/jo302818w | J. Org. Chem. 2013, 78, 3073−3085

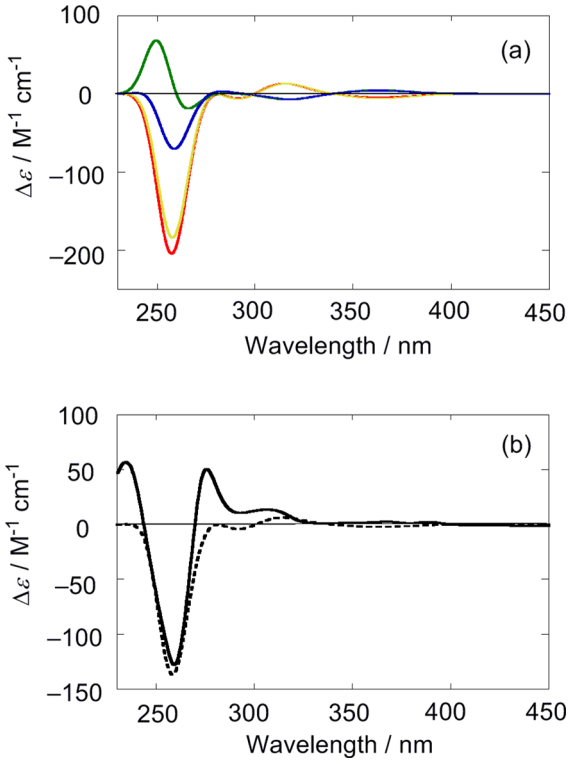

Figure 6. (a) Theoretical CD spectra of the *si*(*anti*) (red), *si*(*g*−) (yellow), *re*(*anti*) (green), and *re*(*g*−) (blue) conformers calculated at the RI-CC2/def2-TZVPP level. (b) Comparison of the theoretical CD spectrum (dotted line), obtained by weight-averaging the component spectra shown in Figure 6a, with the experimental CD spectrum (solid line) measured for a mixture of AC (0.15 mM) and TKS (0.15 mM) in CH_2Cl_2 at 25 °C; the experimental CD intensity ($\Delta\varepsilon$) was corrected for the concentration of AC-TKS complex (0.041 mM) under the conditions employed.

the ^1L_a and ^1L_b bands, respectively. In contrast, the CD spectrum calculated for the *re*(*anti*) conformer was weaker in intensity, opposite in sign, and different in shape from those of the *si*(*anti*/*g*−) conformers, while the *re*(*g*−) conformer exhibited a weaker ^1B_b band and oppositely signed ^1L_a and ^1L_b bands. These component spectra calculated for the individual conformers were weight-averaged on the basis of the conformer population calculated by the SCS-MP2/COSMO method to give the theoretical CD spectrum shown in Figure 6b (dotted line), which is in reasonable agreement in shape and intensity with the experimental CD spectrum (solid line) of the AC-TKS complex measured in dichloromethane. The less perfect matching of the theoretical versus experimental CD spectrum, in comparison with those of AC-AN cross-dimer **5**, is likely to originate from the conformational flexibilities in the weakly bound AC-TKS complex, which allows appreciable contribution of more or less twisted, off-equilibrium conformations energetically achievable at ambient temperatures.

Relative Abundance of *re* and *si* AC-TKS Complexes. As described above, the DFT calculations predicted that the *si* complex is more stable than the *re* complex and the *si*/*re* ratio will be 2.0 in dichloromethane (SCS-MP2/COSMO) at 25 °C, which is opposite to the previous proposal based on an incomplete conformer search.[6b] Hence, we wanted to experimentally verify the preferred formation of the *si* complex by quantitatively analyzing the fluorescence titration behavior at different wavelengths. First, the existence of two fluorescing AC-TKS species was (re)confirmed by fluorescence spectral and lifetime examinations as well as the time-resolved emission spectroscopy (TRES); see Table S4, Figures S14 and S15, and the relevant discussion in the Supporting Information. In the previous study,[6b] we showed that excited *re* and *si* complexes (*re** and *si**) fluoresce at longer and shorter wavelengths, relative to free AC. However, estimating the *si**/*re** ratio directly from the relative fluorescence intensity is not feasible, simply because the fluorescence efficiencies are not necessarily the same for *re** and *si**. In the present study, the relative fluorescence efficiency was evaluated by numerically adjusting the relative contribution of *re** and *si** in the least-squares fitting of the fluorescence titration data so as to match the association constant *K* derived therefrom with that determined independently by a CD spectral titration.[6b]

The fluorescence spectral titration experiment was run at 25 °C by adding various amounts (0−80 equiv) of TKS to a dichloromethane solution of 25 μM AC to give the series of fluorescence spectra shown in Figure 7. The new band

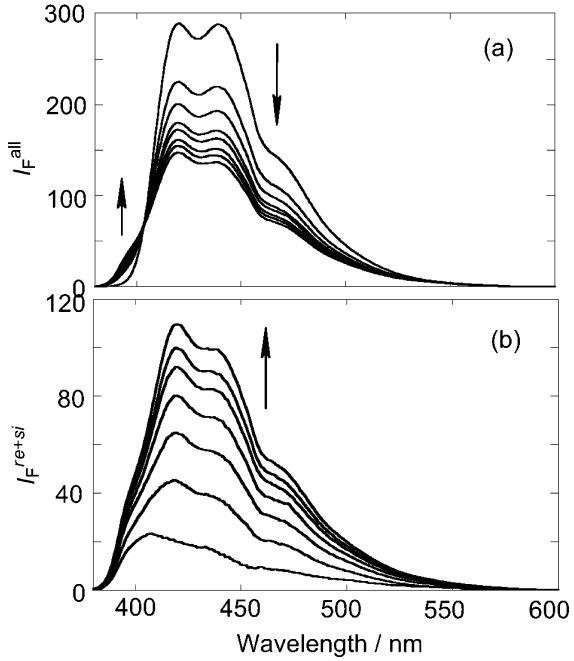

Figure 7. (a) Fluorescence spectra of a dichloromethane solution of 25 μM AC (λ_{ex} 361 nm, the isosbestic point) upon addition of 0, 5.3, 10.7, 18.7, 26.7, 40.0, 53.3, and 80 equiv (0−2.0 mM) of TKS at 25 °C. (b) Net fluorescence spectra of *re* and *si* AC-TKS complexes obtained by subtracting the contribution of free AC fluorescence from the original spectra (a), where the amount of free AC was calculated by using the overall association constant K = 3400 M^{-1} determined by CD spectral titration.[6b]

emerging at shorter wavelengths (<400 nm) and the slowly decreasing emission tail at longer wavelengths (>480 nm) were assigned to the short-lived *si** and the long-lived *re** complex, respectively.[6b] The distinct difference in fluorescence wavelength between *re** and *si** is a reflection of their excited-state structures, since the excitation spectra monitored at 395 and 530 nm were identical with each other in shape and also superimposable with the UV/vis spectrum of AC (Figure S16 in the Supporting Information). In this connection, it is crucial that the fluorescence 0−0 band of anthracenecarboxylic acid appears at 420 nm but blue-shifts to 395 nm upon

dx.doi.org/10.1021/jo302818w | J. Org. Chem. 2013, 78, 3073−3085

deprotonation or a strong hydrogen-bonding interaction.[17] Thus, the *si** species that fluoresces at shorter wavelengths (Figure 7) is likely to be deprotonated or strongly hydrogen-bonded to the pyrrolidine N (for the ground-state structure, see Figure 5a,b) and therefore short-lived. In contrast, the *re** species fluoresces at wavelengths longer than those for free AC, suggesting some extra stabilization through exciplex formation of AC* with the TKS's benzamide moiety (for the ground-state structure, see Figure 5c,d).

In this experiment, the absorbance of AC at the excitation wavelength (361 nm) was kept low at ca. 0.1 and therefore the fluorimeter response was practically proportional to the AC concentration. This allowed us to recover the net fluorescence spectra of *re** and *si** by subtracting the fluorescence attributable to free AC (concentration of which was calculated by using the association constant determined independently)[6b] from the original fluorescence spectrum at each TKS concentration, as shown in Figure 7b.

The fluorescence intensities at 395 and 530 nm (Figure 7b) were plotted against the concentration of TKS to give the apparently smooth titration curves shown in Figure 8 (circle symbols for *re** and triangles for *si**). However, directly fitting the intensity changes at 395 and 530 nm to the 1:1 stoichiometric *re* and *si* complexation leads to erroneous results, because the two equilibria forming *re* and *si* complexes are not independent of each other. Nevertheless, we can assess the relative abundance of *re* and *si* complexes by evaluating the relative fluorescence intensity (α) of *si** monitored at 395 nm and *re** at 530 nm so as to afford the K value consistent with that determined by CD spectral titration (K = 3400 M^{-1}).[6b] After some trials starting with different α values, the modified nonlinear least-squares fit of the fluorescence intensity changes to the 1:1 stoichiometry (Figure 8, solid line) enabled us to determine the α value as 1.7. By using this α value, we calculated the relative abundance of short-lived, more stable *si* complex and long-lived, less stable *re* complex in the presence of a large excess (80 equiv) of TKS as 1.4, which is in reasonable agreement with the value (2.0) predicted by the DFT calculations.

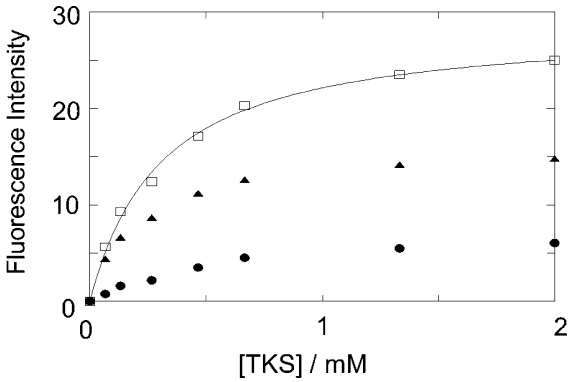

Figure 8. Plots of the fluorescence intensities I_F^{si} at 395 nm, which is assignable solely to the short-lived *si* complex (triangles), I_F^{re} at 530 nm, which is assignable solely to the long-lived *re* complex (circles), and $I_F^{si} + \alpha I_F^{re}$ (α = 1.7) (squares) as a function of the concentration of added TKS. The coefficient α is the relative fluorescence efficiency of *si** and *re** complexes at 395 and 530 nm and was determined as 1.7 by fitting the data (solid line) to give such an overall K which is consistent with that obtained by CD spectral titration: i.e., K = 3400 M^{-1}.[6b]

Enantiodifferentiating Cross-Photocyclodimerization of AC-TKS Complex with AN. In the present system, the preferential excitation of AC over AN is readily achievable by irradiating an AC/AN mixture at the absorption edge of AC, while the factors controlling the subsequent AC-AN cross-photocyclodimerization versus AC-AC homo-photocyclodimerization are not immediately clear. Another interesting feature of this competitive cross-/homo-photocyclodimerization system is the enantiodifferentiation mechanism, which is somewhat complicated upon homo-photocyclodimerization of *re* and *si*-AC TKS complexes, involving not only the route to chiral dimers **2** and **3** but also the "escape" route to achiral dimers **1** and **4**,[6b] but is much more straightforward upon cross-photocyclodimerization affording single chiral dimer **5**.

We first performed the TKS-mediated photocyclodimerization of AC at 25 °C in the presence of varying amounts (0−10 equiv) of AN under the conditions where AC was almost completely (>99%) complexed with TKS (300 equiv) to obtain both homo-dimers **1**−**4** and cross-dimer **5** in the relative yields and ee's shown in Table 3; for representative chiral HPLC charts, see Figure S17 in the Supporting Information. It is interesting that the cross-photocyclodimerization was favored by a factor of 4.3 to give **5** in 81% relative yield even at AN/AC = 1, while the preference was sensibly enhanced up to 44 to afford **5** in 98% yield at AN/AC = 10, enabling us to almost exclusively gain the cross-dimer. Thus, the preference for AC-AN cross-photocyclodimerization was consistently 4.3−4.4 in

Table 3. Enantiodifferentiating Homo- and Cross-Photocyclodimerization of AN and AC Complexed with TKS at Various Temperatures[a]

					product distribution/% (*ee*/%)[d]				
T/°C	TKS/AC[b]	AN/AC	irradiation time/h	AC conversion/%[c]	**1**	**2**	**3**	**4**	**5**
25	300	0	0.5	9	35	28 (−28)	25 (−29)	12	*e*
		1	0.5	10	7	5 (−27)	5 (−26)	2	81 (−22)
		10	0.5	11	0.8	0.5 (*f*)	0.6 (*f*)	0.3	98 (−24)
0	70	1	1	11	7	4 (−34)	4 (−35)	2	83 (−21)
−25	20	1	2	13	6	4 (−40)	5 (−43)	2	83 (−21)
−50	20	1	4	11	7	4 (−44)	6 (−49)	3	80 (−23)

[a]Conditions: irradiated at 390 ± 10 nm under N_2 in a 1 cm cell by a 300 W Xe lamp fitted with an interference filter; [AC] = 0.1 mM in CH_2Cl_2. Under the conditions employed, practically no (<0.3%) photocyclodimerization of AN (0.1 mM) was observed, due not only to the extremely low absorbance at 390 nm but also to the shorter lifetime (2.3 ns) of AN. [b]At the TKS/AC ratios employed, >99% of AC was complexed with TKS at each temperature. [c]Consumption of AC determined by monitoring the UV/vis spectral change at 390 nm. [d]Error in distribution ±1%; error in ee ±3%. [e]Not applicable. [f]Not determined due to low yield.

dx.doi.org/10.1021/jo302818w | J. Org. Chem. 2013, 78, 3073−3085

the competition experiments. Possessing two fully open aromatic faces, AN is inherently two times more advantageous (as a substrate to be attacked by excited AC-TKS complex) than the AC-TKS complex that possesses only one open face. The additional 2.2-fold enhancement may be ascribed to the sterically less hindered open face of AN and/or to the electronically favored formation and cyclodimerization of AN-AC exciplex (with some charge-transfer nature) rather than AC-AC excimer. The faster reaction of AN with the excited AC-TKS complex may also account for the slightly higher conversions observed in the presence of AN (Table 3).

Temperature Effects on Cross/Homo Ratio. In order to elucidate the influence of temperature on the homo/cross ratio and the ee's of homo- and cross-dimers, the competitive cross/homophotocyclodimerization of an equimolar AC/AN mixture was run at temperatures down to −50 °C in the presence of an sufficient amount of TKS to fully (>99%) bind the AC in the system. In these experiments, the conversion (consumption of AC) was kept low at around 10% to avoid any significant deviation from the initial stoichiometry.

As shown in Table 3, the cross/homo-dimer ratio, i.e. **5**/(**1** + **2** + **3** + **4**), was kept nearly constant at 4.5 ± 0.5 over the entire temperature range examined, despite the fact that the conversion, or overall reaction rate, was considerably reduced (by a factor of 7.3) by lowering the temperature from 25 to −50 °C. From the Eyring equation $\ln k = -\Delta H^{\ddagger}/RT + \Delta S^{\ddagger}/R$ (where R is the gas constant) and the 7.3-fold acceleration by increasing the temperature (T) from −50 to 25 °C, the activation enthalpy ($\Delta H^{\ddagger}$) was calculated as 3.5 kcal mol^{-1} for both of the cross- and homo-photocyclodimerizations. On the other hand, the nearly constant cross/homo ratios over the entire temperature range indicate that the high cross/homo selectivity is not enthalpic but exclusively entropic in origin. By further assuming that the product ratio **5**/(**1** + **2** + **3** + **4**) is equal to the relative cross-/homo-photocyclodimerization rate constant k_{cross}/k_{homo}, we obtain the following differential Eyring equation: $\ln(k_{cross}/k_{homo}) = -\Delta\Delta H^{\ddagger}_{cross\text{-}homo}/RT + \Delta\Delta S^{\ddagger}_{cross\text{-}homo}/R$. The plot of ln ($k_{cross}/k_{homo}$), or ln [**5**/(**1** + **2** + **3** + **4**)], as a function of reciprocal temperature gave a flat straight line, as shown in Figure 9. From the slope and intercept of the regression line, we obtain the differential activation parameters $\Delta\Delta H^{\ddagger}_{cross\text{-}homo}$ = 0.1 ± 0.3 kcal mol^{-1} and $\Delta\Delta S^{\ddagger}_{cross\text{-}homo}$ = 3.5 ± 1.0 cal mol^{-1} K^{-1}. These values reveal that the cross-photocyclodimerization is favored solely by the positive entropy, part (1.4 cal mol^{-1} K^{-1}) of which is immediately assignable to the two open faces available for AN (versus the only one open face for AC bound to TKS, which entropically contributes by a $\Delta\Delta S^{\ddagger}$ value of R ln 2 = 1.4 cal mol^{-1} K^{-1}), and the rest is attributable to the steric effects arising from the less hindered AN face rather than the electronic effects, such as the charge-transfer interaction between the AC and AN moieties in an exciplex, which would lead to different enthalpic gains upon cross- and homo-photocyclodimerization.

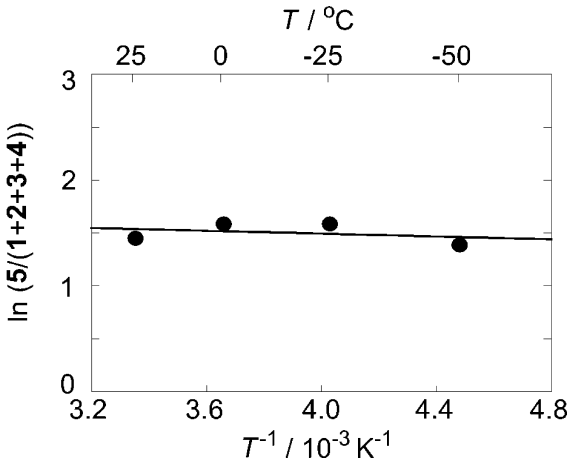

Figure 9. Eyring plot for the homo- and cross-photocyclodimerization of AN and AC bound to TKS.

Temperature Effects on the Enantioselectivities of Cross- and Homo-Dimers. As was the case with the cross-/homo-dimer ratio discussed above, the ee of cross-dimer **5** was kept constant at −22 ± 1% over the entire temperature range employed. However, the ee's of homo-dimers **2** and **3** were noticeably enhanced from −27(±1)% to −47(±2)% by lowering the temperature to −50 °C (Table 3). This incoherent temperature-dependence behavior reveals the complicated nature of the enantiodifferentiation mechanism operative in this mixed photocyclodimerization system, which is likely to involve multiple parameters of different temperature dependencies.

In discussing the enantiodifferentiation mechanism in this competitive photocyclodimerization system, it is essential that all of the favored enantiomers of **2**, **3**, and **5**, each of which elutes as the second fraction under our chiral HPLC conditions, have the same *P* absolute configuration and the two chiral homo-dimers are given in practically the same ee. The former result indicates that the photocyclodimerizations of excited *re* AC-TKS complex with another *re* complex (affording (*P*)-**2** and (*P*)-**3**) and also with AN (affording (*P*)-**5**) are thermodynamically and/or kinetically favored over the reactions of the *si* complex (leading to *M* dimers). The ee's of homo-dimers **2** and **3** were appreciably higher than that of cross-dimer **5** at all the temperatures examined, which is however a natural consequence of the difference in formation mechanism of homo- versus cross-dimer. In the enantiodifferentiating photocyclodimerization of AC mediated by TKS, the enantiomer ratio (er) of chiral **2** and **3** is not a direct function of the relative abundance of the *re*/*si* complexes ([*re*]/[*si*]) but is given as a product of the relative reactivity (k_{re}/k_{si}) and the relative abundances of ground-state complexes ([*re*]/[*si*]) and excited complexes ([*re**]/[*si**]):

$$er_{homo} = (k_{re}/k_{si})([re]/[si])([re^*]/[si^*]) \quad (1)$$

Since the fluorescence excitation spectra monitored at 390 nm (*si** fluorescence) and 530 nm (*re** fluorescence) agreed well with each other and also with the UV/vis spectrum, indicating identical absorption spectra for *re* and *si* complexes, we may assume that $[re^*]/[si^*] = [re]\tau_{re}/[si]\tau_{si}$, where τ_{re} and τ_{si} represent the lifetimes of *re** and *si**, respectively:

$$er_{homo} = (k_{re}/k_{si})(\tau_{re}/\tau_{si})([re]/[si])^2 \quad (2)$$

It is of note that the ee's of homo-dimers **2** and **3** are proportional to the *square* of the relative abundance of *re*/*si* complexes in the ground state. This is because only homochiral *re*-*re* and *si*-*si* cyclodimerizations afford chiral **2** and **3**,[6b] while heterochiral *re*-*si* and *si*-*re* cyclodimerizations lead to achiral **1** and **4**. Due to the existence of this "escape" route to achiral products, the er's of chiral homo-dimers are exaggerated by a factor of [*re*]/[*si*] than the original *re*/*si* ratio achieved upon AC-TKS complex formation in the ground state. In contrast, no

dx.doi.org/10.1021/jo302818w | J. Org. Chem. 2013, 78, 3073−3085

Table 4. Ground-State Population, Fluorescence Lifetime (τ), Enantiomer Ratio (er), and Relative Rate Constants (k_{re}/k_{si}, k_{re}'/k_{si}') for Homo- and Cross-Photocyclodimerization of *re* and *si* Complexes

	population/%[a]			τ/ns[b]			er[c]			
temp/°C	*re*	*si*	[*re*]/[*si*]	*re**	*si**	τ_{re}/τ_{si}	homo	cross	k_{re}/k_{si}[d] (homo)	k_{re}'/k_{si}'[d] (cross)
25	33	67	0.49	4.6	1.6	2.9	1.6	1.6	2.3	1.1
0	32	68	0.47	11.1	4.3	2.6	1.9	1.5	3.3	1.2
−25	30	70	0.43	14.7	4.7	2.6	2.2	1.5	4.6	1.3
−50	28	72	0.39	18.8	7.0	2.7	2.8	1.6	6.8	1.5

[a]Boltzmann distribution based on the energy difference (ΔE) between the *re* and *si* complexes in the ground state, which was calculated by the SCS-MP2/COSMO method. [b]Fluorescence lifetimes of excited *re* and *si* AC-TKS complexes (*re** and *si**) measured by the single-photon-counting method under conditions identical with those for the photoreaction. [c]Experimental (*P*/*M*) enantiomer ratios of the homo- and cross-dimers; the er value for the homo-dimer was obtained by averaging those of **2** and **3**. [d]Relative rate constant for homo- or cross-photocyclodimerization of *re** and *si** with AC or AN, calculated by using eqs 2 and 3, respectively.

such trick exists in the cross-photocyclodimerization, and hence the er of the cross-dimer is linearly proportional to the original *re*/*si* ratio and the relative rate constant k_{re}'/k_{si}', which differs from that for the homophotocyclodimerization:

$$\mathrm{er}_{\mathrm{cross}} = (k_{re}'/k_{si}')(\tau_{re}/\tau_{si})([re]/[si]) \quad (3)$$

For determining the relative rate constants k_{re}/k_{si} and k_{re}'/k_{si}' at different temperatures, we measured the fluorescence lifetimes (τ_{re} and τ_{si}) of *re* and *si* AC-TKS complexes under the same conditions (in temperature and AC and TKS concentrations but without AN) as that employed for the photoreaction, since the excited AC-TKS complex is known to be dynamically quenched by excess TKS in solution.[6b] As shown in Table 4, both τ_{re} and τ_{si} were significantly elongated by lowering the temperature, but interestingly the τ_{re}/τ_{si} ratio was practically kept constant at 2.7 ± 0.1 over the entire temperature range employed. By using eqs 2 and 3, we calculated the relative rate constants k_{re}/k_{si} and k_{re}'/k_{si}' for homo- and cross-photocyclodimerization at each examined temperature, as shown in Table 4.

The relative rate constants k_{re}/k_{si} and k_{re}'/k_{si}' thus obtained were subjected to the Eyring analyses using eq 4, where

$$\ln(k_{re}/k_{si}) = -\Delta\Delta H^{\ddagger}_{re\text{-}si}/RT + \Delta\Delta S^{\ddagger}_{re\text{-}si}/R \quad (4)$$

$\Delta\Delta H^{\ddagger}_{re\text{-}si}$ and $\Delta\Delta S^{\ddagger}_{re\text{-}si}$ denote the differential enthalpy and entropy of activation for the *re**-*re* versus *si**-*si* homocyclodimerization or for the *re**−AN versus *si**−AN cross-cyclodimerization. The differential Eyring plots (Figure 10) afforded good straight lines for both the homo- and cross-photocyclodimerizations. From the slopes and intercepts of the straight lines in Figure 10, we obtained the $\Delta\Delta H^{\ddagger}_{re\text{-}si}$ and $\Delta\Delta S^{\ddagger}_{re\text{-}si}$ values for the homo- and cross-photocyclodimerization, which are listed along with the $T\Delta\Delta S^{\ddagger}_{re\text{-}si}$ and differential free energy of activation $\Delta\Delta G^{\ddagger}_{re\text{-}si}$ values at 25 and −50 °C in Table 5.

It is sensible that both of the $\Delta\Delta H^{\ddagger}_{re\text{-}si}$ and $\Delta\Delta S^{\ddagger}_{re\text{-}si}$ values, sharing the same sign, are significantly larger in the absolute sense for homo- than for cross-photocyclodimerization, since the transition state for the former is highly likely to be sterically more hindered than the latter. The negative $\Delta\Delta H^{\ddagger}_{re\text{-}si}$ and $\Delta\Delta S^{\ddagger}_{re\text{-}si}$ values obtained indicate that the *re* complex is enthalpically more favored by 1.9 and 0.5 kcal mol^{-1} upon homo- and cross-photocyclodimerization, respectively, than the *si* complex, which is however entropically offset at least in part to afford modest $\Delta\Delta G^{\ddagger}_{re\text{-}si}$ values of −0.5 kcal mol^{-1} at 25 °C and −0.9 kcal mol^{-1} at −50 °C for homo-photocyclodimerization and is almost canceled out to give nearly zero $\Delta\Delta G^{\ddagger}_{re\text{-}si}$ values (at both 25 and −50 °C) for cross-photocyclodimerization (Table 5).

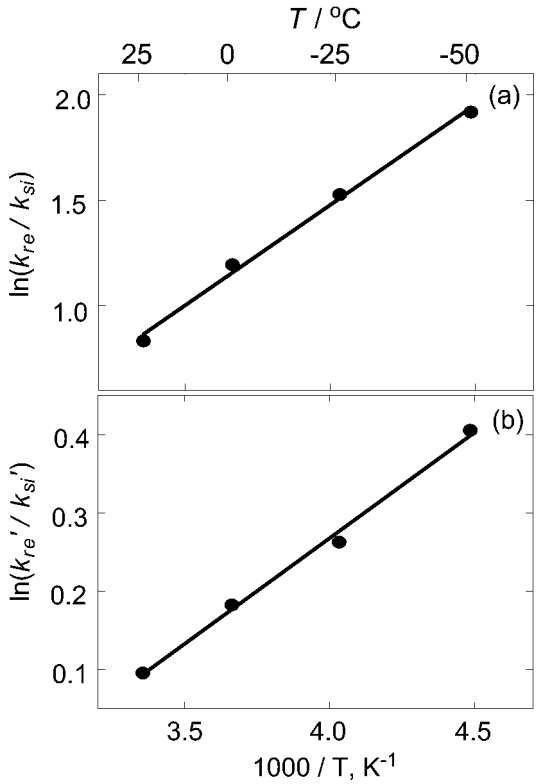

Figure 10. Differential Eyring plots of the relative rate constants (a) k_{re}/k_{si} for homophotocyclodimerization and (b) k_{re}'/k_{si}' for cross-photocyclodimerization. For the original data, see Table 4.

The thermodynamic, kinetic, and activation parameters summarized in Tables 4 and 5 allow us to more closely discuss the mechanisms and factors that govern the enantiodifferentiating homo- and cross-photocyclodimerization of ACs and of AC with AN mediated by TKS and further reveal somewhat unexpected photochirogenic behavior. It is unquestionable that the product's ee is controlled not only by the relative abundance of *re*/*si* AC-TKS complexes ([*re*]/[*si*]) but also by the relative lifetime (τ_{re}/τ_{si}) and rate constant (k_{re}/k_{si}) of excited *re*/*si* complexes in this supramolecular photochirogenic system. It is worth emphasizing that the factor dominating this supramolecular photochirogenic system is not the ground-state thermodynamics, favoring *si*, but the excited-state kinetics (lifetime and reaction rate), both favoring *re*. Thus, the *si* complex is formed more abundantly by a factor of 2.0−2.6 in

dx.doi.org/10.1021/jo302818w | J. Org. Chem. 2013, 78, 3073−3085

Table 5. Differential Activation Parameters for Enantiodifferentiating Homo-Photocyclodimerization of AC-TKS Complex and Cross-Photocyclodimerization of AC-TKS Complex with AN

cyclodimerization mode	temp/°C	$\Delta\Delta H^{\ddagger}_{re\text{-}si}$/kcal mol^{-1}	$\Delta\Delta S^{\ddagger}_{re\text{-}si}$ /cal mol^{-1} K^{-1}	$T\Delta\Delta S^{\ddagger}_{re\text{-}si}$ /kcal mol^{-1}	$\Delta\Delta G^{\ddagger}_{re\text{-}si}$ /kcal mol^{-1}
homo (AC-AC)		−1.9	−4.6		
	25			−1.4	−0.5
	−50			−1.0	−0.9
cross (AC-AN)		−0.5	−1.6		
	25			−0.5	0.0
	−50			−0.4	−0.1

the ground state, whereas the *re** complex has 2.7-fold longer lifetimes and greater rate constants by a factor of 2.3−6.8 (upon reaction with AC) or 1.1−1.5 (upon reaction with AN) to kinetically overwhelm the thermodynamic disadvantage, affording second-eluted (*P*)-**2**, -**3**, and -**5**.

It is also true that the conflicting ground-state thermodynamics and excited-state kinetics are responsible for the moderate ee's obtained in this homo-/cross-photocyclodimerization system. This finding, however, provides us a clue for improving the stereochemical outcome of templated supramolecular photochirogenesis in general. In the present case, if the original preference for *si* upon ground-state complexation with TKS is not offset but amplified by the excited-state lifetime and reactivity (or alternatively the *re* preference in the excited state is further augmented), substantial synergistic enhancement of enantioselectivity will be achieved. In this context, it is constructive to discuss the origin(s) of the longer lifetime and higher reactivity of the *re** over the *si** complex. The longer lifetime and the red-shifted fluorescence of the *re** complex, which indicates stabilization, are most likely to originate from the more π-overlapped conformation of the *re* complex in the ground state (Figures 5c,d) that facilitates exciplex formation upon excitation. In contrast, the *si** complex is short-lived and fluoresces at shorter wavelengths than for *re** and AC*, indicating destabilization relative to free AC*, probably because the AC in the *si** complex, being not well π-overlapped with the TKS's benzamide moiety in the ground state (Figures 5a,b), more strongly interacts with the pyrrolidine N through hydrogen-bonding/electrostatic interactions, developing a more negative charge on AC to show blue-shifted, short-lived fluorescence. The higher reactivity of the *re** complex may also originate from the charge-transfer nature of the exciplex intermediate, which makes the AC* moiety more electron-deficient to facilitate the photocyclodimerization of the *re** complex with both AC and AN through an acceptor−donor−donor triplex-like transition state. These considerations provide us with some practical strategies for better manipulating the excited-state lifetime and reactivity of the *si* complex that is favored in the ground state, for example, by (1) introducing bulky substituent(s) to the benzamide moiety to destabilize the more π-overlapped *re* complex in both ground and excited states, (2) modifying the prolinol tether, and/or (3) extending the TKS's aromatic system to enhance the π overlap with the AC in the *si** complex.

CONCLUSIONS

In this mechanistic study on the first enantiodifferentiating cross-photocyclodimerization of anthracenes, we have developed a set of theoretical and experimental tools for analyzing the ground- and excited-state behavior of chiral species intervening in the enantiodifferentiating cross-/homo-photocyclodimerization of AC and AN mediated by a chiral hydrogen-bonding template. In elucidating the detailed mechanisms, the comparative examinations of the homo- and cross-photocyclodimerizations were indispensable for more straightforward and consistent analyses of the inherent enantioselectivities upon ground-state complexation and excited-state cyclodimerization, and also for more detailed evaluation of the electronic and steric effects that control the ground-state thermodynamics and excited-state kinetics operative in this enantiodifferentiating photocyclodimerization.

One of the most interesting features of this supramolecular photochirogenic system is the significant acceleration of the cross-photocyclodimerization by a factor of ca. 4 (irrespective of the irradiation temperature), 2 of which is simply due to the statistics (two available faces for AN but just one for the AC-TKS complex). Another 2-fold enhancement is almost entirely entropic in origin ($\Delta\Delta H^{\ddagger}_{\text{cross-homo}}$ = 0.1 kcal mol^{-1} and $\Delta\Delta S^{\ddagger}_{\text{cross-homo}}$ = 3.5 cal mol^{-1} K^{-1}), probably attributable to the less hindered AN face. It is also interesting mechanistically, and a bit frustrating synthetically, that the ground-state thermodynamics (*re*/*si* complex ratio) does not play the major role in this chiral template-mediated photochirogenesis but is overwhelmed by the excited-state kinetics (lifetime and rate constant, which are synergistic with each other). This is certainly a drawback in getting higher ee but will be overcome by exploiting the strategies proposed above at the end of the last section. Investigations along this line are currently in progress.

EXPERIMENTAL SECTION

General Considerations. Mass spectra were obtained by fast atom bombardment on a double-focusing mass spectrometer. ^{1}H NMR spectra at 600 MHz, ^{13}C NMR spectra at 150 MHz, and COSY, NOESY, HSQC, and HMBC spectra at 600 MHz were obtained in DMSO-d_6. UV/vis spectra were recorded on a spectrophotometer equipped with a temperature controller and circular dichroism (CD) spectra on a spectropolarimeter equipped with a temperature controller. Fluorescence spectra were recorded on a spectrofluorimeter with excitation and emission slits of 1 and 3 nm, respectively; the excitation wavelength was set at 361 nm, the isosbestic point observed upon UV/vis spectral titration of AC with TKS. Fluorescence lifetimes were determined by the single photon counting method. In the time-resolved emission spectrum (TRES) measurement, the fluorescence decays upon excitation at 361 nm were collected for 20 min at room temperature from 380 to 600 nm at every 5 nm (Figure S14 in the Supporting Information).

Materials. Commercially available reagent-grade anthracene (AN), 2-anthracenecarboxylic acid (AC), fluorescence-free dichloromethane, and methanol were used without further purification. Acetonitrile for HPLC analysis was distilled prior to use. The chiral hydrogen-bonding template 4-amino-5-chloro-2-methoxy-*N*-((2*S*,4*S*)-1-ethyl-2-hydroxymethyl-4-pyrrolidinyl)benzamide (TKS159) was prepared as reported previously.[18]

Sample Preparation. Stock solutions of AC and AN (0.8 mM) were prepared by dissolving appropriate amounts of AC and AN in dichloromethane, and the final concentrations were fine-adjusted to

dx.doi.org/10.1021/jo302818w | J. Org. Chem. 2013, 78, 3073−3085

0.8 mM by further diluting the solution with the same solvent with UV monitoring at 397 nm (ε 4100 M^{-1} cm^{-1}) for AC and at 378 nm (ε 7000 M^{-1} cm^{-1}) for AN. Stock solutions of TKS at 0.64, 4, 14, 20, and 60 mM concentrations were prepared by dissolving the exact amounts of TKS in dichloromethane. For the cross-photocyclodimerization of AC with AN in the presence of varying amounts of TKS, the stock solutions (0.5 mL each) of AC and AN at 0.8 mM and that of TKS (2 mL) at 0.64, 4, 14, or 60 mM were mixed and the resulting solution was diluted with 1 mL of dichloromethane to make a series of sample solutions containing AC (0.1 mM), AN (0.1 mM), and TKS (0.32, 2, 7, 10, and 30 mM). The sample solution thus prepared was transferred to a quartz cell (10 × 10 × 40 mm), purged with nitrogen gas for 5 min in ice water, sealed with a septum cap, and then subjected to the photoirradiation with stirring in a cryostat at a given temperature.

UV/vis spectrum of isolated *rac*-**5** (25 μM) was recorded in a 1:1 mixture of acetonitrile and a 10 mM aqueous solution of NaOH.

The dichloromethane solutions of AC (25 μM) containing 20 mM TKS were prepared for TRES, fluorescence lifetime, and fluorescence and excitation spectra measurements of *re*/*si* AC-TKS complexes (Table S4 and Figures S14−S16 in the Supporting Information).

Photoirradiation and Product Analyses. A 500 W ultrahigh-pressure mercury−xenon lamp fitted with a UV-35 filter (effective λ >320 nm) and a 300 W xenon lamp fitted with an interference filter (360, 390, or 400 ± 10 nm) were used as light sources. All irradiations were run in a cryostat (with a magnetic stirrer) maintained at a given temperature (±1 °C). After irradiation, the solvent was removed in vacuo, the residue obtained was dissolved in a mixture of acetonitrile and aqueous 2 mM NaOH solution (2 mL each), and the resulting solution was subjected to chiral HPLC analysis.

Product analyses were performed on an HPLC system equipped with a tandem column of Cosmosil 5C18-AR-II (Nacalai) and Chiralcel OJ-RH (Daicel), which was eluted with a water/acetonitrile mixture containing 0.1% trifluoroacetic acid (TFA) at a flow rate of 0.5 mL min^{-1} at 35 °C; the product distribution and the peak areas relative to the remaining AC did not appreciably vary after the irradiated sample stood at 35 °C for several hours in the dark, indicating that the cyclodimers are totally stable at that temperature. The composition of the eluent was varied from CH_3CN/H_2O = 30/70 to 80/20 with a gradient of 10% h^{-1}. An aliquot of 5 μL was injected to HPLC, and the product distribution and ee were determined from the peak areas of the chromatogram monitored by a fluorescence detector (excitation at 254 nm and monitoring at 420 nm)[13] and occasionally by a circular dichroism detector (monitoring at 254 nm). The fluorescence response of cross-dimer **5**, relative to homo-dimers **1**−**4**, was calibrated by comparing the peak areas monitored by the fluorescence detector for the solutions of **1** and **5** at known concentrations: [**1**] = 10.7, 5.3, and 1.07 μM, [**5**] = 25, 12.5, and 5.0 μM.

Preparative-Scale Irradiation and the Isolation and Enantiomer Separation of Cross-Dimer 5. A methanol solution (400 mL) of 1.1 mM AC (100 mg, 0.45 mmol) and 2.2 mM AN (160 mg, 0.90 mmol) was placed in a doughnut-shaped Pyrex vessel, purged with nitrogen, and then irradiated for 2 h at room temperature with a 300 W high-pressure mercury lamp fitted with a uranium glass sleeve (effective wavelength >320 nm). At the end of irradiation, 97% of AC was consumed, as judged from the absorbance change at 400 nm (Figure S8 in the Supporting Information). The photolyzed solution was evaporated in vacuo to give a residue (258 mg), part of which was subjected to preparative HPLC on a Sumipax ODS JP column (Sumika, 6 μm, 20 mm i.d. × 25 cm) eluted with water/acetonitrile/TFA (45/55/0.1) at a flow rate of 5 mL min^{-1} to give pure cross-dimer **5** (3 mg). *rac*-**5**: ^{1}H NMR (600 MHz, DMSO-d_6) δ 12.64 (br s, 1H, COOH), 7.52 (s, 1H), 7.46 (d, J = 7.4 Hz, 1H), 7.06 (d, J = 7.4 Hz, 1H), 6.96 (m, 6H), 6.79 (m, 6H), 4.73 (d, J = 11.2 Hz, 1H), 4.72 (d, J = 11.2 Hz, 1H), 4.66 (d, J = 11.2 Hz, 1H), 4.65 (d, J = 11.2 Hz, 1H); ^{13}C NMR (150 MHz, DMSO-d_6) δ 167.3 (C═O), 148.9, 144.0, 143.4, 143.3, 143.2, 143.2, 143.2, 142.8, 127.5, 126.8, 126.9, 126.8, 126.8, 126.7, 126.7, 125.3, 125.3, 125.3, 125.2, 125.2, 52.3, 52.2, 52.1, 52.1; HR-MS (FAB, negative) [M − H$^-$] m/z 399.1402 ($C_{29}H_{19}O_2^-$ requires 399.1391); error +4.3 ppm/+1.1 mmu.

rac-**5** thus isolated was subjected to preparative chiral HPLC on a Daicel Chiralcel OJ-RH column (5 μm, 20 mm i.d. × 25 cm) eluted with water/acetonitrile/TFA (50/50/0.1) at a flow rate of 5 mL min^{-1} to give the first and second fractions that contained $\mathbf{5}_+$ and $\mathbf{5}_-$, respectively; note that the subscripts + and − do not mean dextro- and levorotatory but just indicate the order of elution on the chiral column used; the absolute configurations were determined by the comparison of experimental and theoretical CD spectra (vide infra). These fractions were directly subjected to UV/vis and CD spectral examinations.

Fluorescence Spectral Titration for Determining Relative Fluorescence Efficiency and Abundance of *re* and *si* Complexes. Fluorescence spectral titration was performed to determine the relative abundance of diastereomeric *re*- and *si*-AC-TKS complexes by gradually adding a dichloromethane solution of TKS (20 mM) to a dichloromethane solution (3 mL) of AC (0.025 mM) at 25 °C, where the absorbance at the excitation wavelength (361 nm) was 0.094−0.11 and hence the detector response was proportional to the AC concentration, which allowed us to correct the spectra for the dilution upon titration. The net fluorescence spectra of diastereomeric AC-TKS complexes were obtained by spectrum subtraction of the contribution of free AC (concentration of which was calculated by using the association constant K (3400 M^{-1}) determined by the conventional CD spectral titration) from the corrected fluorescence spectrum at each TKS concentration. Since the *re* and *si* AC-TKS complexes show distinctly different fluorescence lifetimes (10.0 and 3.7 ns, respectively, at 25 °C) and fluorescence spectra,[6b] the relative contribution of *re* and *si* complexes can be evaluated by analyzing the fluorescence intensity changes measured at the wavelength specific to each complex.

Theoretical Calculations. All the calculations were performed on Linux-PCs with the TURBOMOLE 6.2 program suite.[19] The geometry of AC-AN cross-dimer **5** was optimized at the DFT-D2-B97-D/TZVP level[20] with numerical quadrature grid m4. The 12 possible conformers of stacked AC-TKS complexes were geometry-optimized at the DFT-D3-B-LYP/def2-TZVP level with a zero-damping function[21] and finer grid of m5. A single-point energy calculation[16] was consecutively run for each optimized structure by using the SCS-MP2 method with the basis set of def2-TZVPP, and the effect of solvent was checked by using the conductor-like screening model (COSMO) with dielectric constant set to 8.93 for dichloromethane.[15] The Boltzmann distribution based on the relative energy thus obtained gave the conformer population in the ground state. All excited-state calculations were performed on the optimized ground-state geometries and were simulated by the time-dependent approximate coupled cluster linear response (RI-CC2)[22] method with the basis-set def2-TZVPP quality for both AC-AN dimer **5** and AC-TKS complexes. We chose the values from the reportedly robust length-gauge representations for the rotatory and oscillator strengths. The CD spectra were simulated by overlapping the Gaussian functions for each transition, where the bandwidth at 1/e height is fixed at 0.4 eV. The spectra were red-shifted by 0.2 eV in the case of anthracene photodimer **5**, since there were systematic errors in theoretical transition energies, mostly due to the incompleteness of basis sets in our calculations.[9] In all calculations, we employed the resolution of the identity approximation for the Coulomb part. For the results of the conformation search of AC-TKS complexes, see Figure S12 in the Supporting Information.

■ ASSOCIATED CONTENT

Supporting Information

Figures, tables, and text giving HR-MS, 1D- and 2D-NMR, UV/vis, and CD spectra of cross-dimer **5**, UV/vis spectral changes upon irradiation of the AC/AN/TKS mixture, fluorescence detector calibration, DFT-D3 calculation results (energies and geometries), fluorescence spectra and lifetimes, and TRES results. This material is available free of charge via the Internet at http://pubs.acs.org.

AUTHOR INFORMATION

Corresponding Author

*E-mail for Y.I.: inoue@chem.eng.osaka-u.ac.jp.

Notes

The authors declare no competing financial interest.

ACKNOWLEDGMENTS

This work was supported by the Japan Society for the Promotion of Science (Grants-in-Aid for Scientific Research No. 24655029, 23750129, 23350018, and 21245011), which are gratefully acknowledged.

REFERENCES

(1) (a) Griesbeck, A. G.; Meierhenrich, U. J. *Angew. Chem., Int. Ed.* **2002**, *41*, 3147. (b) Inoue, Y., Ramamurthy, V., Eds. *Chiral Photochemistry*; Marcel Dekker: New York, 2004. (c) Müller, C.; Bach, T. *Aust. J. Chem.* **2008**, *61*, 557. (d) Hoffmann, N. *Chem. Rev.* **2008**, *108*, 1052.

(2) Yang, C.; Inoue, Y. Supramolecular Photochirogenesis. In *Supramolecular Photochemistry*; Ramamurthy, V., Inoue, Y., Eds.; Wiley: Hoboken, NJ, 2011; pp 115−154.

(3) Sivaguru, J.; Natarajan, A.; Kaanumalle, L. S.; Shailaja, J.; Uppili, S.; Joy, A.; Ramamurthy, V. *Acc. Chem. Res.* **2003**, *36*, 509−521.

(4) (a) Bach, T.; Bergmann, H.; Harms, K. *Angew. Chem., Int. Ed.* **2000**, *39*, 2302−2304. (b) Bach, T.; Bergmann, H.; Grosch, B.; Harms, K. *J. Am. Chem. Soc.* **2002**, *124*, 7982−7990. (c) Bauer, A.; Weskamper, F.; Grimme, S.; Bach, T. *Nature* **2005**, 1139−1140. (d) Müller, C.; Bauer, A.; Maturi, M. M.; Cuquerella, M. C.; Miranda, M. A.; Bach, T. *J. Am. Chem. Soc.* **2011**, *133*, 16689−16697.

(5) Cauble, D. F.; Lynch, V.; Krische, M. J. *J. Org. Chem.* **2003**, *68*, 15−21.

(6) (a) Mizoguchi, J.; Kawanami, Y.; Wada, T.; Kodama, K.; Anzai, K.; Yanagi, T.; Inoue, Y. *Org. Lett.* **2006**, *8*, 6051−6054. (b) Kawanami, Y.; Pace Tamara, C. S.; Mizoguchi, J.; Yanagi, T.; Nishijima, M.; Mori, T.; Wada, T.; Bohne, C.; Inoue, Y. *J. Org. Chem.* **2009**, *74*, 7908−7921. (c) Kawanami, Y.; Katsumata, S.; Mizoguchi, J.; Nishijima, M.; Fukuhara, G.; Yang, C.; Mori, T.; Inoue, Y. *Org. Lett.* **2012**, *14*, 4962−4965.

(7) (a) Nakamura, A.; Inoue, Y. *J. Am. Chem. Soc.* **2003**, *125*, 966−972. (b) Nakamura, A.; Inoue, Y. *J. Am. Chem. Soc.* **2005**, *127*, 5338−5339. (c) Ke, C.; Yang, C.; Mori, T.; Wada, T.; Liu, Y.; Inoue, Y. *Angew. Chem., Int. Ed.* **2009**, *48*, 6675−6677.

(8) (a) Wada, T.; Nishijima, M.; Fujisawa, T.; Sugahara, N.; Mori, T.; Nakamura, A.; Inoue, Y. *J. Am. Chem. Soc.* **2003**, *125*, 7492−7493. (b) Nishijima, M.; Wada, T.; Mori, T.; Pace, T. C. S.; Bohne, C.; Inoue, Y. J. *Am. Chem. Soc.* **2007**, *129*, 3478−3479. (c) Fuentealba, D.; Kato, H.; Nishijima, M.; Fukuhara, G.; Mori, T.; Inoue, Y.; Bohne, C. J. *Am. Chem. Soc.* **2013**, *135*, 203−209.

(9) Wakai, A.; Fukasawa, H.; Yang, C.; Mori, T.; Inoue, Y. *J. Am. Chem. Soc* **2012**, *134*, 4990−4997.

(10) (a) Berlman, I. B. *Handbook of Fluorescence Spectra of Aromatic Molecules*; Academic: New York, 1971; p 356. (b) Murov, S. L.; Carmichael, I.; Hug, G. L. *Handbook of Photochemistry*, 2nd ed.; Marcel Dekker: New York, 1993; p 7.

(11) Qiu, H.; Yang, C.; Inoue, Y.; Che, S. *Org. Lett.* **2009**, *11*, 1793−1796.

(12) Bailey, D.; Williams, V. E. *J. Org. Chem.* **2006**, *71*, 5778−5780.

(13) Nishijima, M.; Wada, T.; Nagamori, K.; Inoue, Y. *Chem. Lett.* **2009**, *38*, 726−727.

(14) (a) Wallwe, M. P.; Kruse, H.; Mück-Lichtenfeld, C.; Grimme, S. *Chem. Soc. Rev.* **2012**, *41*, 3119−3128. (b) Grimme, S. *Angew. Chem., Int. Ed.* **2008**, *47*, 3430−3434. (c) Goerigk, L.; Grimme, S. *Phys. Chem. Chem. Phys.* **2011**, *13*, 6670−6688. (d) Grimme, S. *Chem. Eur. J.* **2012**, *18*, 9955−9964.

(15) Klamt, A.; Jonas, V. *J. Chem. Phys.* **1996**, *105*, 9972−9981.

(16) (a) Grimme, S. *J. Chem. Phys.* **2003**, *118*, 9095−9102. (b) Grimme, S. *J. Phys. Chem. A* **2005**, *109*, 3067−3077.

(17) Milosavljevic, B. H.; Thomas, J. K. *J. Phys. Chem.* **1988**, *92*, 2997−3001.

(18) Yanagi, T.; Katajima, A.; Anzai, K.; Kodama, K.; Mizoguchi, J.; Fujiwara, H.; Sakiyama, H.; Kamoda, O.; Kamei, C. *Chem. Pharm. Bull.* **1999**, *47*, 1650−1654.

(19) TURBOMOLE V6.2 (2010), product of University of Karlsruhe and Forschungszentrum Karlsruhe GmbH in 1989−2007 and of TURBOMOLE GmbH since 2007; http://www.turbomole.com.

(20) Grimme, S. *J. Comput. Chem.* **2004**, *25*, 1463−1473.

(21) (a) Liu, Y.; Goddard, W. A., III *Mater. Trans.* **2009**, *50*, 1664−1670. (b) Moellmann, J.; Grimme, S. *Phys. Chem. Chem. Phys.* **2010**, *12*, 8500−8504. (c) Hujo, W.; Grimme, S. *Phys. Chem. Chem. Phys.* **2011**, *13*, 13942−13950.

(22) Christiansen, O.; Koch, H.; Jorgensen, P. *Chem. Phys. Lett.* **1995**, *243*, 409−418.